

# The PANDA DIRC Detectors

E. Etzelmüller<sup>e,\*</sup>, J. Schwiening<sup>a,\*</sup>, A. Ali<sup>a,b</sup>, A. Belias<sup>a</sup>, R. Dzhygadlo<sup>a</sup>, A. Gerhardt<sup>a</sup>, M. Krebs<sup>a,1</sup>, D. Lehmann<sup>a</sup>, K. Peters<sup>a,b</sup>, G. Schepers<sup>a</sup>, C. Schwarz<sup>a</sup>, M. Traxler<sup>a</sup>, L. Schmitt<sup>c</sup>, M. Böhm<sup>d</sup>, A. Lehmann<sup>d</sup>, M. Pfaffinger<sup>d</sup>, S. Stelter<sup>d</sup>, F. Uhlig<sup>d</sup>, M. Düren<sup>e</sup>, K. Föhl<sup>e</sup>, A. Hayrapetyan<sup>e</sup>, K. Kreutzfeld<sup>e</sup>, J. Rieke<sup>e</sup>, M. Schmidt<sup>e</sup>, T. Wasem<sup>e</sup>, C. Sfiuti<sup>f</sup>

<sup>a</sup>GSI Helmholtzzentrum für Schwerionenforschung GmbH, Darmstadt, Germany

<sup>b</sup>Goethe University, Frankfurt a.M., Germany

<sup>c</sup>FAIR, Facility for Antiproton and Ion Research in Europe, Darmstadt, Germany

<sup>d</sup>Friedrich Alexander-University of Erlangen-Nuremberg, Erlangen, Germany

<sup>e</sup>II. Physikalisches Institut, Justus Liebig-University of Giessen, Giessen, Germany

<sup>f</sup>Institut für Kernphysik, Johannes Gutenberg-University of Mainz, Mainz, Germany

---

## Abstract

The PANDA experiment at the future Facility for Antiproton and Ion Research (FAIR) will address fundamental questions of hadron physics with unprecedented precision. To reach this goal excellent Particle Identification (PID) is essential over a large range of particle momenta and solid angles. Most of the phase space will be covered by two innovative DIRC (Detection of Internally Reflected Cherenkov light) detectors. The Endcap Disc DIRC and Barrel DIRC will cover the polar angle range from 5 to 22° and 22 to 140°, respectively. Both detectors rely on high precision optical components, lifetime-enhanced Microchannel Plate PMTs (MCP-PMTs), and fast readout electronics.

**Keywords:** Cherenkov Detector; DIRC; Particle Identification; MCP-PMT

---

## 1. PANDA at FAIR

The PANDA (AntiProton Annihilation at Darmstadt) experiment will be one of the four pillars of the future Facility for Antiproton and Ion Research (FAIR) which is currently under construction at Gesellschaft für Schwerionenforschung (GSI) in Darmstadt, Germany. Antiprotons with momenta ranging from 1.5 to 15 GeV/c will collide with a fixed proton or hypernuclear target to study various topics involving weak and strong forces, exotic states, and the structure of hadrons. The PANDA detector will provide precise tracking, energy measurement, and efficient particle identification (PID). PID of charged hadrons in the target spectrometer of the PANDA experiment will be realized primarily by two DIRC counters: the Endcap Disc DIRC for polar angles between 5 and 22° and the Barrel DIRC for angles between 22 and 140° (see Fig. 1).

## 2. DIRC principle

In contrast to conventional Ring Imaging Cherenkov (RICH) detectors, which use gas or aerogel to produce the Cherenkov light, DIRC detectors are based on solid radiator materials, in the form of bars or plates, with a much higher refractive index. This allows to operate the RICH technology in a region of lower particle momenta and enables the construction of thin detectors with a depth of only few centimeters along the particle

trajectory. The key technology of each DIRC is the fabrication of highly parallel and precisely polished optical surfaces which conserve the Cherenkov angle information during total internal reflection, which traps part of the produced Cherenkov photons and guides them towards the readout region. For this purpose synthetic fused silica is typically used for the radiator due to its radiation hardness and machinability. The detection of the Cherenkov light is based on single photon sensors which, in the case of PANDA, must provide a high lifetime, radiation hardness and have to work inside a magnetic field of up to 1 T in the readout region.

## 3. The PANDA Endcap Disc DIRC

### 3.1. Detector Design

The Endcap Disc DIRC (EDD) will provide particle identification of charged pions from kaons for momenta up to 4 GeV/c with a separation power of at least 3 standard deviations. Covering the forward endcap region of the PANDA experiment, the requirements for the detector differ from other designs to date. The detector is divided into four independent quadrants which together form a dodecagon with a central rhombic opening for the acceptance of the PANDA Forward Spectrometer. Each quadrant consists of a radiator and 24 Readout Modules (ROMs). Each ROM contains three bars, three Focusing Elements (FELs), a Microchannel Plate Photomultiplier Tube (MCP-PMT), and a Frontend Electronics board (see also Fig. 2).

Radiator, bars, and FELs form the optical system of the detector and are made of synthetic fused silica. The thickness of

---

\*Corresponding authors

Email addresses:

erik.etzelmue@exp2.physik.uni-giessen.de (E. Etzelmüller),

j.schwiening@gsi.de (J. Schwiening)

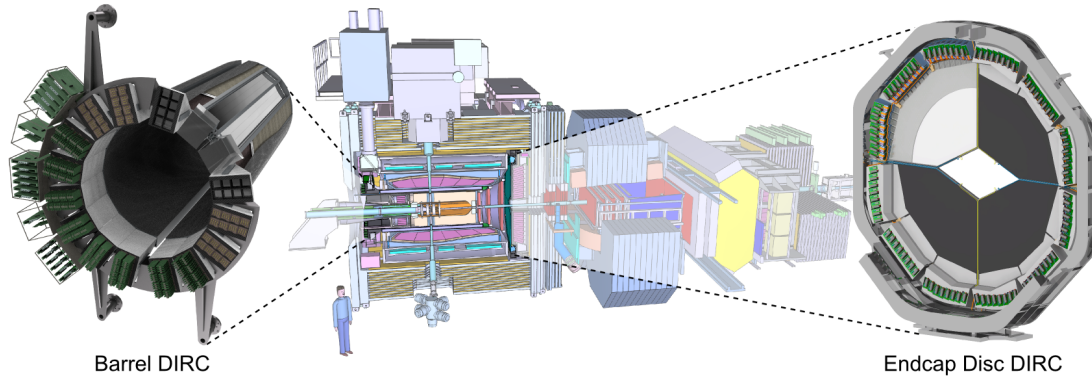


Figure 1: Side view of the PANDA experiment, highlighting the locations of the two DIRC detectors.

a radiator amounts to 20 mm at a maximum diameter of 1.5 m. To minimize photon loss and conserve the angle information the surface roughness is below 1 nm RMS with a Total Thickness Variation (TTV) below  $15 \mu\text{m}$ . For manufacturing reasons, and due to space limitations, the bars extend the radiator volume. They will be glued to the outer rim of the radiator plate in order to avoid the need for optical in situ alignment and to reduce the needed mechanical support structure. To improve the focusing quality and reduce photon loss the coupling of the bars and FELs is done via optical contact bonding. The FELs transform the angle information into a position information by internally focusing the Cherenkov photons via an aluminum coated cylindrical surface (see Fig. 3).

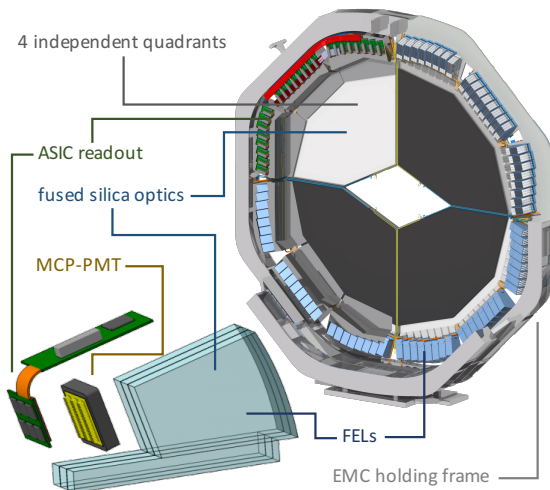


Figure 2: CAD image of the complete Endcap Disc DIRC and the inside of a Readout Module (ROM), indicating key components.

The shape of the FELs is optimized to match the resolution of the MCP-PMTs, which have a pitch size of 0.5 mm or smaller, and at the same time align them with respect to the magnetic field of roughly 0.8 T to provide sufficient gain for single photon detection. The MCP-PMTs are 2-inch tubes with a customized anode containing either  $3 \times 100$  or  $6 \times 128$  pixels. Measurements inside a magnetic field have shown that charge sharing between adjacent pixels will only occur at the edges of the pix-

els as the (secondary) photoelectrons are guided by the magnetic field lines [1].

In order to extend the life time of the MCP-PMTs, which is proportional to the accumulated charge on the photocathode, which can reach  $7 \text{ C/cm}^2$  or more during the lifetime for the EDD, and to mitigate the contribution of the chromatic error, a long pass wavelength filter will be applied. Simulations have shown that an optimal cut-off wavelength is at around 350 nm which can be realized either by an optical filter in front of the MCP-PMT or a modified photocathode [2].

The analog single photon signal originating from the MCP-PMTs will be readout and digitized by the TOFPET2 ASIC by PETsys with 64 channels per ASIC [3]. The ASICs will be bonded to a flex PCB which forms the Frontend Electronics Board together with an FPGA and a versatile link option. In total the system will be able to readout a maximum of 36,864 channels.

### 3.2. Reconstruction and Performance

The reconstruction of the Cherenkov angle is based on a three dimensional measurement: the pixel position on the MCP-PMT ( $z(\phi')$ ), the position of the FEL and the time of propagation. The latter is not used directly in the reconstruction algorithm but resolves ambiguities of overlapping patterns. The resolution of  $z(\phi')$  is limited by the pixel size and the resolution of the FELs as well as the width of the bars as indicated in Fig. 3 (b) as the exact azimuthal position of the Cherenkov light entering the bar is unknown.

Taking into account the momentum vector of the particle emitting the Cherenkov photons, the Cherenkov angle can be calculated analytically for each pixel hit. On average 22 photons are detected for each charged particle track. For geometrical reasons the performance depends on the particle track position and ranges between 1.1 and 2.2 mrad at 4 GeV/c which translates into a separation power between 3 and 6 standard deviations [4].

### 3.3. Prototype Results

In the course of the development of the detector, individual prototypes of all previously described detector components have been produced and tested including custom made setups for quality assurance and assembly [1, 5].

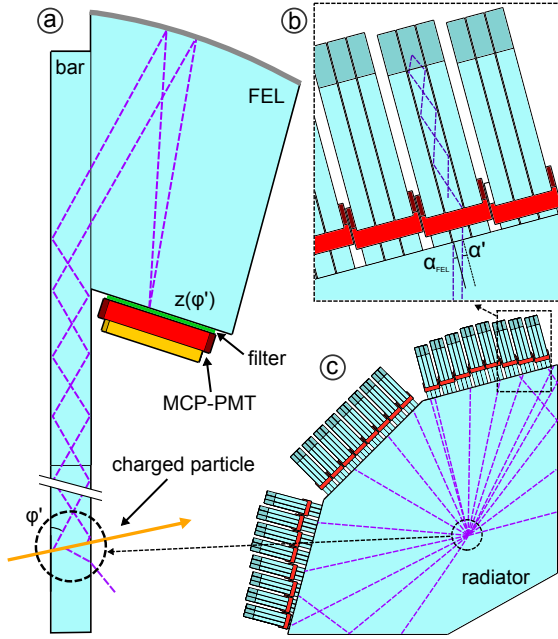


Figure 3: (a) A charged particle traverses the radiator and emits Cherenkov photons (dashed lines). Photons which fulfill the condition for total internal reflection propagate towards the ROMs where they enter a bar and subsequently a Focusing Element (FEL) where they are focused on a MCP-PMT. (b) The azimuthal angle is determined from the position of the bar where the photon enters the ROMs. (c) shows different light paths inside the radiator.

Since 2015 all detector prototypes, which were tested in hadron and electron beams at CERN and DESY, consisted of a  $500 \times 500 \times 20 \text{ mm}^3$  radiator, focusing optics made of synthetic fused silica, and high-resolution MCP-PMTs. The readout electronics and mechanics were improved for each test beam campaign, featuring a TOFPET2 ASIC readout and 3D-printed ROM mechanics in the latest version.

Because of the reduced size of the radiator and the limited number of available ROMs for the EDD prototype, the analysis of the test beam data focused on the single photon resolution (SPR) and photon yield, comparing them to Monte Carlo predictions (see Fig. 4 (a)). The Monte Carlo data can subsequently be extrapolated from the test beam geometry to the final geometry. A SPR value of 6.06 mrad, measured using a 3 GeV/c electron beam at DESY in 2016, corresponds to a SPR for pions in the full EDD detector of 1.8 mrad at the same momentum [4]. Another approach was taken for the so called combined event analysis, where the data taken during a vertical scan for a single FEL was combined to simulate a prototype equipped with 30 FELs (or 10 ROMs). For each combined event the photon yield and the average so-called track resolution was calculated and compared to Monte Carlo predictions. Fig. 4 (b) and (c) show the good agreement between the test beam data and the simulation with a measured combined track resolution of 2.52 mrad (2.18 mrad for the Monte-Carlo simulation) [6].

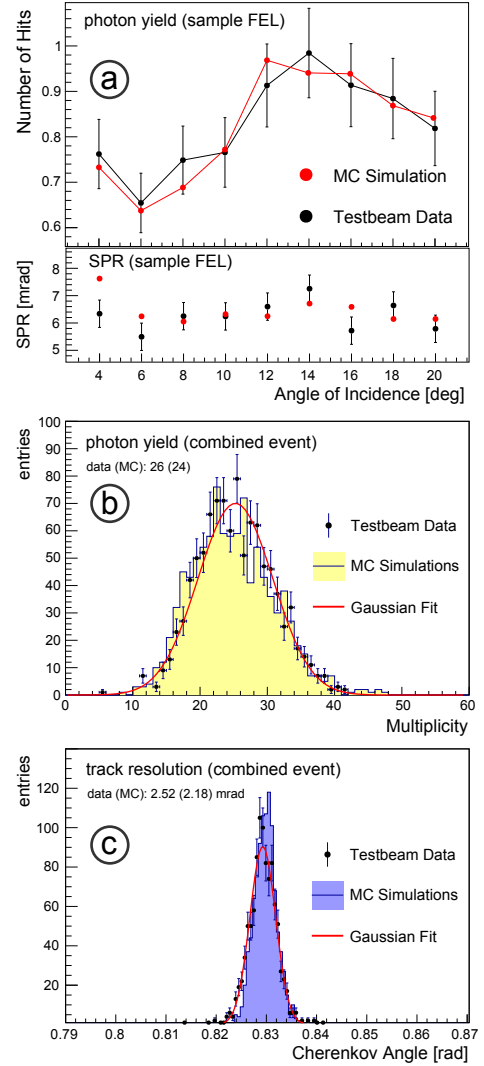


Figure 4: (a) photon yield and single photon resolution (SPR) for a single FEL for an electron beam at DESY during the 2016 test beam campaign. (b) and (c) show the photon yield and track resolution for the combined event analysis, respectively.

## 4. The PANDA Barrel DIRC

### 4.1. Detector Design

The Barrel DIRC is designed to provide clean separation of charged pions from kaons with 3 standard deviations or more for momenta up to 3.5 GeV/c. The concept, shown in Fig. 5, is based on the successful BaBar DIRC detector [8] as well as key results from the R&D for the SuperB FDIRC [9], with several important improvements, such as fast photon timing and a compact imaging region.

The design is described in detail in the Technical Design Report [7]. Sixteen optically isolated sectors, each comprising a bar box and a synthetic fused silica prism, surround the beam line in a 16-sided polygonal barrel with a radius of 476 mm. Each bar box contains three synthetic fused silica bars of 17 mm thickness, 53 mm width, and 2400 mm length, placed side-by-side, separated by a small air gap. A flat mirror is attached to the

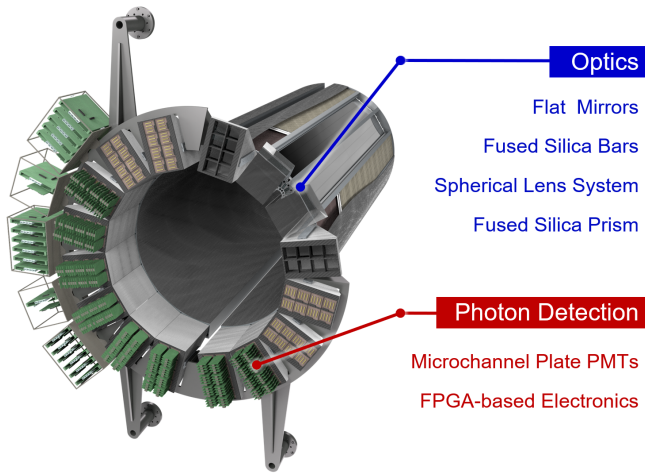


Figure 5: Schematic of the PANDA Barrel DIRC.

forward end of each bar to reflect photons towards the readout end, where they are focused by a 3-layer spherical lens on the back of a 300 mm-deep solid prism, made of synthetic fused silica, serving as expansion volume (EV). An array of  $2 \times 4$  lifetime-enhanced MCP-PMTs [10], each with  $8 \times 8$  pixels of about  $6.5 \times 6.5 \text{ mm}^2$  size, is placed at the back surface of the prisms to detect the photons and measure their arrival time on a total of 8192 pixels with a precision of about 100 ps in the magnetic field of approximately 1 T.

The readout of the MCP-PMTs is based on the TRB-technology [11], combined with the FPGA-based DiRICH front-end amplification and discrimination module [12]. The MCP-PMTs are mounted on a highly-integrated backplane, which provides the high voltage to the sensors as well as low voltages and signal routing to the DiRICH cards. By measuring the photon arrival time as well as the Time-over-Threshold of the signal, the performance of the sensors can be monitored and time-walk effects can be corrected, improving the precision of the single photon timing.

All major mechanical components will be built from aluminum alloy and Carbon-Fiber-Reinforced Polymer (CFRP) to minimize the material budget and weight and to maximize the stiffness.

The PANDA Barrel DIRC will be the first DIRC counter utilizing lens focusing. The innovative design of the optics produces a flat image, matching the shape of the back surface of the fused silica prism. This is achieved by a combination of focusing and defocusing elements in a spherical triplet lens made from one layer of lanthanum crown glass between two layers of synthetic fused silica. This 3-layer lens works without any air gaps, minimizing the photon loss that would otherwise occur at the transition from the lens to the expansion volume.

#### 4.2. Reconstruction and Performance

The performance of the PANDA Barrel DIRC design was evaluated using a detailed physical simulation, implemented in Geant4 [13], and validated using complex prototypes in particle beams at GSI and CERN. The Geant simulation is tuned to

wavelength-dependent properties of the materials used and the most important Cherenkov photon loss processes: the photon transport efficiency during total internal reflections [14] and the quantum and collection efficiency of MCP-PMTs [15].

Two reconstruction approaches were developed to evaluate the detector performance [16]. The geometrical reconstruction is based on the approach used by the BaBar DIRC [8]. The value of the Cherenkov angle of each detected photon is reconstructed using the relative position of the bar and the MCP-PMT pixel, in combination with the particle direction, and PID is performed in a track-by-track maximum likelihood test. The algorithm can also determine the Cherenkov angle per particle and the photon yield, as well as the single photon Cherenkov angle resolution, important figures of merit in evaluating the performance of a prototype design in test beams and comparing it to other Cherenkov detectors. While the geometrical method relies primarily on the position of the detected photons, the time-based imaging approach, based on the method used by the Belle II TOP [17], utilizes both the position and time information with comparable precision, and directly performs the maximum likelihood test based on the photon arrival time in each pixel.

#### 4.3. Prototype Results

The performance of a number of PANDA Barrel DIRC system prototypes, featuring different radiator and prism geometries, focusing options, and readout electronics, was determined using particle beams at GSI and CERN from 2011–2017 to validate the design and the simulation results.

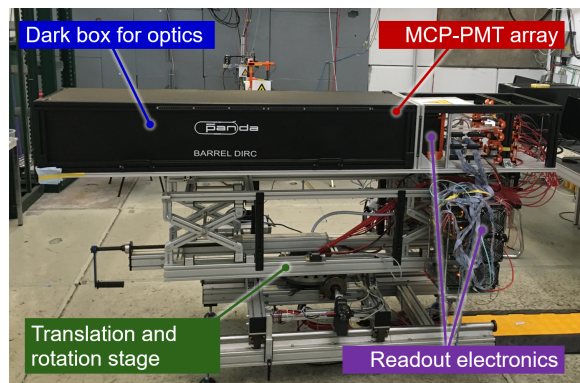


Figure 6: Photograph of the 2017 prototype in the CERN T9 beam line.

The prototype tested at the T9 beamline at the CERN PS in 2017, shown in Fig. 6, featured all critical elements of the final PANDA Barrel DIRC design: A narrow fused silica radiator bar ( $17.1 \times 35.9 \times 1200.0 \text{ mm}^3$ ) coupled on one end to a flat mirror, on the other end to a 3-layer spherical focusing lens, a fused silica prism as expansion volume (with a depth of 300 mm and a top angle of  $38^\circ$ ), an array of  $2 \times 4$  MCP-PMTs, and 600 readout electronics channels using TRBs in combination with FPGA-based amplification and discrimination cards (PADIWA) [18], mounted directly on the MCP-PMTs.

The time difference measured by two time-of-flight stations was used to cleanly tag an event as pion or as proton. The experimental data showed good agreement of the Cherenkov hit

patterns with simulation, both in the pixel space and in the photon hit time space.

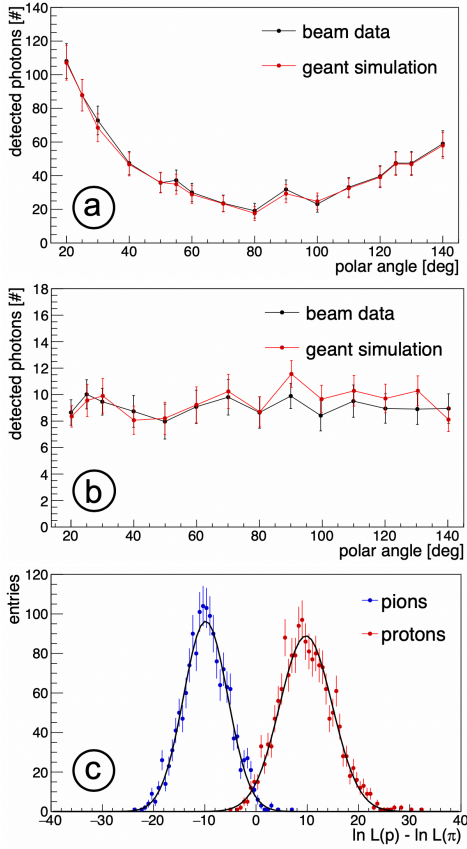


Figure 7: Performance of the PANDA Barrel DIRC prototype at the CERN PS in 2017 for a beam momentum of 7 GeV/c.

Photon yield (a) and single photon Cherenkov angle resolution (SPR) (b) from the geometric reconstruction as a function of the track polar angle for tagged protons. The error bars correspond to the RMS of the distribution in each bin. Proton-pion log-likelihood difference distributions (c) for proton-tagged (red) and pion-tagged (blue) beam events from time-based imaging reconstruction for a polar angle of 20°.

Examples of the performance of the PANDA Barrel DIRC prototype with a narrow bar and a 3-layer spherical lens at the CERN PS in 2017 are shown in Fig. 7. For tagged protons at 7 GeV/c momentum the number of Cherenkov photons ranges from 20 to 110 and the single photon Cherenkov angle resolution (SPR) varies between 8–11 mrad, both in good agreement with simulation. The log-likelihood difference distributions obtained using time-based imaging reconstruction for tagged pions and protons with a polar angle of 20° and a momentum of 7 GeV/c is shown in Fig. 7 (c). The separation power determined from the Gaussian fits is  $4.2 \pm 0.1$  s.d., corresponding to a  $\pi/K$  separation power of  $4.4 \pm 0.1$  s.d. at a momentum of 3.5 GeV/c. Simulation can be used to extrapolate this value to the performance of the fully equipped PANDA Barrel DIRC. Assuming that the expected technical specifications of the MCP-PMTs, lenses, and readout electronics, in particular the photon detection efficiency and timing precision, are achieved as planned, the result extrapolates to a  $\pi/K$  separation power of about 7.7 s.d. at 25° and 3.5 GeV/c in PANDA,

exceeding the PANDA PID requirements.

## 5. Summary and Outlook

The PANDA Endcap Disc DIRC and the Barrel DIRC have shown significant progress over the past few years. The technical designs were completed and the performance of prototypes validated with complex prototypes in particle beams at CERN and DESY. Both DIRC detectors are now transitioning to the construction phase with component fabrication starting in early 2019 and installation into PANDA scheduled for 2023/2024, followed by commissioning with protons soon after and first physics with antiprotons in 2025.

## Acknowledgements

This work was supported by the Bundesministerium für Bildung und Forschung (BMBF), HGS-HIRe, HIC for FAIR, and by the EIC detector R&D (eRD14) fund, managed by Brookhaven National Lab. We thank GSI, DESY and CERN staff for the opportunity to use the beam facilities and for their on-site support as well as the RICH2018 organizers in Moscow for an outstanding meeting.

- [1] J. Rieke, et al., *Resolution changes of MCP-PMTs in magnetic fields*, *JINST* **11** (2016) C05002.
- [2] M. Düren, et al., *The Endcap Disc DIRC of PANDA*, *Nucl. Instr. and Meth. Res. Sect. A* **876** (2017) 198.
- [3] A. Di Francesco, et al., *TOFPET2: a high-performance ASIC for time and amplitude measurements of SiPM signals in time-of-flight applications*, *JINST* **11** (2016) C03042.
- [4] M. Schmidt, et al., *Particle identification algorithms for the PANDA Endcap Disc DIRC*, *JINST* **12** (2017) C12051.
- [5] E. Etzelmüller, et al., *Tests and developments of the PANDA Endcap Disc DIRC*, *JINST* **11** (2016) C04014.
- [6] K. Föhl, et al., *The PANDA Endcap Disc DIRC*, *JINST* **13** (2018) C02002.
- [7] PANDA Collaboration, *Technical Design Report for the PANDA Barrel DIRC Detector*, *J. Phys. G: Nucl. Part. Phys.*, <https://doi.org/10.1088/1361-6471/aade3d>.
- [8] I. Adam et al., *The DIRC particle identification system for the BaBar experiment*, *Nucl. Instr. and Meth. Res. Sect. A* **538** (2005) 281.
- [9] D. A. Roberts et al., *Results from the FDIRC prototype*, *Nucl. Instr. and Meth. Res. Sect. A* **766** (2014) 114.
- [10] A. Lehmann et al., *Recent Developments with Microchannel-Plate PMTs*, *Nucl. Instr. and Meth. Res. Sect. A* **876** (2017) 42.
- [11] C. Ugur et al., *264 Channel TDC Platform applying 65 channel high precision (7.2 psRMS) FPGA based TDCs*, 2013 IEEE Nordic-Mediterranean Workshop on Time-to-Digital Converters (NoMe TDC) (2013), doi:10.1109/NoMeTDC.2013.6658234.
- [12] J. Michel et al., *Electronics for the RICH detectors of the HADES and CBM experiments*, *JINST* **12** (2017) C01072.
- [13] S. Agostinelli et al., *Geant4 - a simulation toolkit*, *Nucl. Instr. and Meth. Res. Sect. A* **506** (2003) 250.
- [14] J. Cohen-Tanugi et al., *Optical Properties of the DIRC Fused Silica Cherenkov Radiator*, *Nucl. Instr. and Meth. Res. Sect. A* **515** (2003) 680.
- [15] F. Uhlig et al., *Breakthrough in the lifetime of microchannel plate photomultipliers*, *Nucl. Instr. and Meth. Res. Sect. A* **787** (2015) 105.
- [16] R. Dzhygadlo et al., *Simulation and reconstruction of the PANDA Barrel DIRC*, *Nucl. Instr. and Meth. Res. Sect. A* **766** (2014) 263.
- [17] M. Staric et al., *Pattern recognition for the time-of-propagation counter*, *Nucl. Instr. and Meth. Res. Sect. A* **639** (2011) 252.
- [18] M. Cardinali et al., *Frontend electronics for high-precision single photoelectron timing using FPGA-TDCs*, *Nucl. Instr. and Meth. Res. Sect. A* **766** (2014) 231.